Quantitative CT-based Structural Alterations of Segmental Airways in Cement Dust-Exposed Subjects

Taewoo Kim
Kyungpook National University
Hyun Bin Cho
Kyungpook National University School of Mechanical Engineering
Woo Jin Kim
Kangwon National University Hospital Department of Internal Medicine and Environmental Health Center
Chang Hyun Lee
Seoul National University College of Medicine Department of Radiology
Kum Ju Chae
Chonbuk National University Hospital Biomedical Research Institute
So-Hyun Choi
Kyungpook National University Department of Statistics
Kyeong Eun Lee
Kyungpook National University Department of Statistics
So Hyeon Bak
Kangwon National University Hospital Department of Internal Medicine and Environmental Health Center
Sung Ok Kwon
Kangwon National University Hospital Department of Internal Medicine and Environmental Health Center
Gong Yong Jin
Chonbuk National University Hospital Biomedical Research Institute
Jiwoong Choi
University of Iowa IIHR Hydroscience and Engineering
Eun-Kee Park
Kosin University College of Medicine Department of Medical Humanities and Social Medicine
Ching-Long Lin
University of Iowa IIHR Hydroscience and Engineering
Eric A Hoffman
The University of Iowa College of Medicine Department of Radiology
Sanghun Choi (s-choi@knu.ac.kr)
Kyungpook National University https://orcid.org/0000-0001-5030-0296

Research

Keywords: airway narrowing, wall thickening, bifurcation angle, stiffness of airway structure, and percent emphysema

Posted Date: May 28th, 2020

DOI: https://doi.org/10.21203/rs.3.rs-16792/v2

Version of Record: A version of this preprint was published at Respiratory Research on May 29th, 2020. See the published version at https://doi.org/10.1186/s12931-020-01399-9.

Abstract

Background: Dust exposure has been reported as a risk factor of pulmonary disease, leading to alterations of segmental airways and parenchymal lungs. This study aims to investigate alterations of quantitative computed tomography (QCT)-based airway structural and functional metrics due to cement-dust exposure.

Methods: To reduce confounding factors, subjects with normal spirometry without fibrosis, asthma and pneumonia histories were only selected, and a propensity score matching was applied to match age, sex, height, smoking status, and pack-years. Thus, from a larger data set (N=609), only 41 cement dust-exposed subjects were compared with 164 non-cement dust-exposed subjects. QCT imaging metrics of airway hydraulic diameter (D_h), wall thickness (WT), and bifurcation angle (θ) were extracted at total lung capacity (TLC) and functional residual capacity (FRC), along with their deformation ratios between TLC and FRC.

Results: In TLC scan, dust-exposed subjects showed a decrease of D_h (airway narrowing) especially at lower-lobes (p<0.05), an increase of WT (wall thickening) at all segmental airways (p<0.05), and an alteration of θ at most of the central airways (p<0.001) compared with non-dust-exposed subjects. Furthermore, dust-exposed subjects had smaller deformation ratios of WT at the segmental airways (p<0.05) and θ at the right main bronchi and left main bronchi (p<0.01), indicating airway stiffness.

Conclusions: Dust-exposed subjects with normal spirometry demonstrated airway narrowing at lower-lobes, wall thickening at all segmental airways, a different bifurcation angle at central airways, and a loss of airway wall elasticity at lower-lobes. The airway structural alterations may indicate different airway pathophysiology due to cement dusts.

Background

Dust exposure has been reported as a risk factor for pulmonary disease. For example, occupational dust exposure has been significantly associated with chronic obstructive pulmonary disease (COPD) (1). Exposure to desert dust has been correlated with an increased risk of hospitalization for asthma (2). An association between dust exposure and lung function has been reported via cytological and spirometry findings. In dusty areas near cement plants, the serum mercury level of blood samples was correlated with a decrease in the forced expiratory volume in one second (FEV_1) and a risk of obstructive lung disease (3). In addition, workers exposed to dust working in a cement factory were likely to have a decrease in peak expiratory flow (4). However, the effects of environmental dust exposure on residents near cement plants have not been studied in detail. In this study, we hypothesize that environmental dust exposure by cements is associated with alterations of quantitative computed tomography (QCT)-based airway structural and functional metrics. Thus, QCT imaging-based variables are used to investigate structural and functional alterations due to dust exposure.

With respect to QCT imaging, few studies have investigated the effects of dust exposure on airway structure and lung function. For instance, coal and gold miners have been found to have a higher prevalence of emphysema compared with control groups (5). The emphysema score measured by QCT has been associated with construction workers who are heavily exposed to asbestos (6) but not quartz and silica (7, 8). Many previous studies have been limited regarding fully understanding the effects of dust exposure because they employed only one or a few imaging variables for a small number of subjects. More recently, Marchetti et al. (9) demonstrated that occupational dust-exposed subjects had a greater percentage of emphysema, percentage of air trapping, and wall

area. The advanced post-processing of QCT imaging can reveal more airway structure features, such as airway luminal hydraulic diameter (D_h), wall thickness (WT), and bifurcation angle (q) in proximal airways, as well as parenchymal functional features, including air volume, tissue volume, the determinant of Jacobian (Jacobian), percent functional small airway disease (fSAD%), and percent emphysema (Emph%), through the image registration technique (10). QCT metrics were able to classify clinically meaningful clusters of asthma (11).

With a comprehensive set of QCT imaging-based metrics, we aim to investigate unique features of airway structure and lung parenchymal function between subjects exposed to cement dust (dust-exposed: DE) and subjects with none or little exposure to cement dust (non-dust-exposed: NDE). The DE and NDE subjects were acquired at two different imaging sites, respectively. Both imaging sites collected two CT images for a subject at functional residual capacity (FRC) and total lung capacity (TLC). To minimize the intersite variability, we employed a fraction-threshold method (10, 12), when estimating parametric response map, i.e., fSAD% and Emph%. Next, to control the intersubject variability due to sex, age, height, smoking history, pack-years, and more, we employed a statistical method, i.e., propensity score matching method (13). This allows for an objective comparison between two groups.

Methods

Due to technological limitations, the Methods section is only available as a download in the supplementary files section.

Results

Demographics information

Table 2 shows the demographic information for DE and NDE subjects in the before- and after- propensity score based matched data. The standardized differences of sex and smoking status were zero, indicating an exact matching. Standardized differences of continuous metrics, i.e., age, height, and pack-years were 1.4, 0.5, and 0.3, respectively. Note that the value of standardized difference smaller than 10 is considered as well-balanced. After matching the continuous metrics, body mass index (BMI) of two groups is also shown to be balanced.

Segmental airways of dust-exposed subjects at TLC and FRC

Fig 3 shows the generational (left column) and regional (middle and right columns) differences in D_h between DE and NDE subjects from TLC scans ($D_{h,\,TLC}$; top row) and FRC scans ($D_{h,\,FRC}$; bottom row). Relative to NDE subjects, the $D_{h,\,TLC}$ and $D_{h,\,FRC}$ of DE subjects were smaller in the airways at RMB, TriLUL, and TriRUL (**Fig 3B and 3E**). The significant difference of D_h was observed especially at all lobes in TLC (P<0.05). Except for these airways, there were no or little statistical difference of the $D_{h,\,TLC}$ and $D_{h,\,FRC}$.

Fig 4 then shows the generational and regional differences of WT from TLC (top row) and FRC (bottom row) scans. DE subjects had increased WT in all regions except for RMB and LMB at the TLC scan and all regions except for LLB6 at the FRC scan. Consequently, WT was significantly increased from 2nd to 5th generation (P<0.001), being different from D_h. Compared with NDE subjects, the θ_{TLC}, and θ_{FRC} of the trachea and TriRUL were increased, and the θ_{TLC} of RMB, LMB, TriLUL and LLB6 was decreased in DE subjects (**Fig 5A, 5B**). Similarly, the θ_{FRC} of DE subjects were decreased in RMB, TriLUL, and LLB6 compared with that of NDE subjects (**Fig 5B**).

Regarding the deformation ratio of D_h (ε^{Dh}), there was no statistical difference between the two groups (not reported here). On the other hand, the ε^{WT} of the 4^{th}-5^{th} generations and all subgrouped lobes except sRUL and sLLL, namely segmental airways, were significantly smaller in DE subjects than NDE subjects (**Fig 6**). Next, DE subjects had significantly smaller ε^{θ} in the RMB, LMB, and TriLUL (**Table 3**). Based upon WT and θ, DE subjects were found to have smaller deformations in bronchial structures when they breathe between TLC and FRC. The quantities possibly indicate an increase in airway stiffness of DE subjects. For instance, **Fig 7** supports this trend of bifurcation angle change at RMB between TLC and FRC in a DE subject (male; 74 years; BMI=28) and an NDE subject (male; 67 years; BMI=25).

Functional features of dust-exposed subjects

Table 4 shows the differences of QCT-based functional metrics between NDE and DE subjects. The values of TLC, FRC, and IC were presented with absolute values, rather than % predicted values, because sex, age, and height of the data were already balanced by PSM method. Regarding air volumes, both TLC and FRC of DE subjects were smaller, and IC was also smaller in DE subjects than those of NDE subjects. The Jacobian indicating volume change ratio was decreased in DE subjects at right upper lobe and right middle lobe, consistent with IC. Emph% of DE subjects was lower than that of NDE subjects. However, fSAD% of DE subjects was not significantly different from that of NDE subjects. A figure was displayed to demonstrate parenchymal features of Emph% and fSAD% (**Fig 8**).

Discussion

In this study, with the aid of advanced QCT imaging analysis, we have investigated alterations of the airway structure and lung function at multiscale levels in subjects exposed to cement dust. Most similar studies (1-5, 8, 9) included patients with pulmonary diseases such as COPD and asthma, whereas for an objective comparison, this study excluded patients with pneumonia, asthma, and COPD to minimize confounding effects due to the pulmonary diseases. We also employed a robust statistical method of propensity score matching to control demographic confounders such as age, sex, height, smoking history, and pack-years. It has been known that imaging protocols between different centers are sensitive when estimating density-based imaging metrics such as Emph%, and fSAD% (22), whereas they are less sensitive on airway size parameters (20). Therefore, we employed a fraction threshold method to compute the Emph% and fSAD%.

With sensitive QCT imaging metrics, we demonstrated that the airway structures of DE subjects had different features from those of NDE subjects. The DE subjects are characterized by phenotypes of airway narrowing (D_h) at lower-lobes, wall thickening (WT) at all segmental airways, and alteration of branching structure (θ) at central airways. These findings were similarly observed in a previous study where individuals with occupational exposure had an increased airway wall thickness (9). In the meantime, a multicenter study of former and current smokers using the multi-ethnic study of atherosclerosis (MESA) COPD data reveals that COPD subjects caused by mainly smoking have thinner airway walls (23). The subjects in this study could be also progressed into COPD later, but these subjects exposed by cement dusts have thickened airway walls. A previous study has reported that exposure to cement dust leads to an increase in airway inflammation (24). Thus, the distinguished phenotypes on airway walls are likely to indicate different airway pathophysiology.

A recent asthma study by Shim et al. (25) using severe asthma research program (SARP) data has demonstrated an association of airway lumen change between TLC and FRC with a corticosteroid treatment, but there were no

investigations of wall thickness and branching angle changes between TLC and FRC. In this study, we computed strains for airway hydraulic diameter, wall thickness, and branching angle. To our best knowledge, this is the first effort of estimating strains at bronchial levels between TLC and FRC. As a result, the DE subjects were found to have the increased stiffness of wall thickness (ε^{WT}) and bifurcation angle (ε^{θ}) which could be affected by lung fibrosis and atelectasis, possibly due to the airway inflammation. In particular, the stiffened airways were likely to affect the prevention of airway deformation from FRC to TLC, sustaining the airway skeletal structure at FRC.

Regarding parenchymal functional variables (**Table 4**), lung volume at TLC, lung volume at FRC, IC, and Jacobian in DE subjects were smaller than NDE subjects. The decreased IC and Jacobian in DE subjects also could indicate a reduction of lung deformation. Especially, the reduction of Jacobian was found to be significantly correlated with e^{q} at RMB (Spearman test R=0.416, P<0.005). Based upon our analysis, we presume that the significantly reduced lung volume at TLC was caused by a reduced volume change (Jacobian). This is also possibly correlated with an increased stiffness of airways estimated by e^{WT} and e^{q} (**Table 3 and Fig 6**). In this study, fSAD% of DE subjects was similar with NDE subject, and Emph% of DE subjects was even lower than NDE subjects (**Table 4**). This is possibly due to the subgrouping by normal lung function, and also indicates that structural alterations of segmental airways begin earlier than parenchymal functional alterations.

Compared with lung functional metrics, airway structural variables provided very clear differences between the DE and NDE subjects. This implies that dust exposure due to cements was significantly associated with bronchial alterations in segmental scales rather than in parenchymal levels. As the size of cement dust ranges from 0.5 to 5 mm (16), cement particles may be deposited in segmental airways (24, 26, 27). These features are different from the characteristics of cigarette smoke particles. Sahu et al. (28) demonstrated that the deposition rate of cigarette smoke particles was greater in parenchymal regions than in segmental regions due to the small size of the particles (ranging from 0.01 to 1 mm). A previous study found that smokers with normal spirometry were more susceptible to parenchymal alteration associated with the emphysema score (29, 30). Whether the structural alterations observed here progress to parenchymal levels, leading to severe air-trapping and emphysema, has yet to be confirmed with a longitudinal study.

This study has several limitations. It was retrospectively designed by utilizing CT images collected at two respective sites. Thus, the findings obtained here were possibly influenced by intersite variability, such as scanner difference. However, as shown in **Table 1**, the two centers used the same scanner make (Siemens), same inspiratory maneuver (TLC), same expiratory maneuver (FRC), and similar reconstruction algorithms (B30f from KNUH and B35f from CNUH), so consistent regional attenuation, airway diameter, and wall thickness between the two groups are expected (31, 32). In addition, the percent emphysema and percent fSAD were derived from the method using a fraction-threshold (10) that is a density variation-free method. Therefore, these results were not significantly influenced by scanner differences. In the previous study (20, 33), we already confirmed that different scanner had little confounding effect for QCT analysis with data derived from different sites. Furthermore, dust-exposed subjects could suffer from several pulmonary diseases such as interstitial lung disease and fibrosis which were not indicated by FEV_1 and FVC. Therefore, it was better to include DLCO for the criterion when choosing subjects with normal lung function. Unfortunately, DLCO was not collected in this project, but we excluded any noticeable parenchymal diseases such as fibrosis, asthma, and pneumonia, so we believe that the current features in cement dust exposed subjects remained the same.

Conclusions

In conclusion, with QCT imaging metrics, we demonstrated that DE subjects had unique features of airway structure, especially in segmental airways, compared with NDE subjects. In structural variables, DE subjects showed airway narrowing at lower-lobes, wall thickening at all segmental airways, a different bifurcation angle at central airways, and a loss of airway wall elasticity at lower-lobes compared with NDE subjects. Unlike segmental airways, parenchymal changes were relatively marginal at this stage for subjects with normal spirometry, which may be associated with the large size of cement dust. It has yet to be investigated if airway structural changes are associated with flow structure and particle distribution and deposition, so a future study with computational fluid dynamics is needed.

Declarations

Ethics Approval and Consent to Participate

Both the KNUH and CNUH studies were approved by the Institutional Review Board at individual sites (KNUH 2019-06-007 and CUH 2016-03-020-005)

Consent for Publication

Not applicable

Availability of Data and Material

Not applicable

Competing Interests

Eric A. Hoffman is a shareholder in VIDA diagnostics, a company that is commercializing lung image analysis software derived by the University of Iowa lung imaging group. He is also a member of the Siemens CT advisory board.

Funding/Support

This study was supported by the Korea Ministry of Environment (MOE) as “The Environmental Health Action Program” [RE201806039, and RE201806027], Basic Science Research Program through the National Research Foundation of Korea funded by the Ministry of Education [NRF-2017R1D1A1B03034157].

Author’s Contributions

Conception and design: T.K., H.B.C., S.C.; acquisition of data: W.J.K., C.H.L., K.J.C., S.H.B., S.O.K., G.Y.J.; analysis and interpretation of data: all authors; drafting the article or revising it critically for important intellectual content: T.K., H.B.C.,S.C., S.H.C., E.A.H., C.L.L.; final approval of the version to be published: all authors.

Acknowledgements

Not applicable

Abbreviations

QCT: Quantitative computed tomography

D_h: Hydraulic diameter

WT: Wall thickness

θ: Bifurcation angle

TLC: Total lung capacity

FRC: Functional residual capacity

COPD: Chronic obstructive pulmonary disease

FEV_1: Forced expiratory volume in one second

Jacobian: Determinant of Jacobian

fSAD%: Percent functional small airway disease

Emph%: Percent emphysema

DE: Dust-exposed

NDE: Non-dust-exposed

KNUH: Kangwon national university hospital

CODA: Chronic obstructive pulmonary disease in dusty areas near cement plants

CNUH: Chonbuk national university hospital

FVC: Forced vital capacity

PSM: Propensity score matching

PFT: Pulmonary function test

BMI: Body mass index

ε^{Dh}: Deformation ratio of D_h

ε^{WT}: Deformation ratio of WT

ε^{θ}: Deformation ratio of θ

RMB: Right main bronchus

LMB: Left main bronchus

RUL: Right upper lobe

RML: Right middle lobe

RLL: Right lower lobe

LUL: Left upper lobe

LLL: Left lower lobe

BronInt: Right intermediate bronchus

TriLLB: Trifurcation of left lower lobe

sRUL: Sub-grouped right upper lobe with branches of RB1 to RB3

sRML: Sub-grouped right middle lobe with branches of RB4 to RB5

sRLL: Sub-grouped right lower lobe with branches of RB6 to RB10

sLUL: Sub-grouped left upper lobe with branches of LB1 to LB5

sLLL: Sub-grouped left lower lobe with branches of LB6, and LB8 to LB10

IC: Inspiratory capacity

SD: Standard deviation

CI: Confidence interval

MESA: Multi-ethnic study of atherosclerosis

SARP: Severe asthma research program

References

1. Fishwick D, Bradshaw LM, D'SOUZA W, Town I, Armstrong R, Pearce N, et al. Chronic bronchitis, shortness of breath, and airway obstruction by occupation in New Zealand. American journal of respiratory and critical care medicine. 1997;156(5):1440-6.
2. Kanatani KT, Ito I, Al-Delaimy WK, Adachi Y, Mathews WC, Ramsdell JW. Desert dust exposure is associated with increased risk of asthma hospitalization in children. American journal of respiratory and critical care medicine. 2010;182(12):1475-81.
3. Heo J, Park HS, Hong Y, Park J, Hong S-H, Bang CY, et al. Serum heavy metals and lung function in a chronic obstructive pulmonary disease cohort. Toxicology and Environmental Health Sciences. 2017;9(1):30-5.

4. Zeleke ZK, Moen BE, Bråtveit M. Cement dust exposure and acute lung function: a cross shift study. BMC pulmonary medicine. 2010;10(1):19.
5. Garshick E, Schenker MB, Dosman JA. Occupationally induced airways obstruction. Medical Clinics. 1996;80(4):851-78.
6. Huuskonen O, Kivisaari L, Zitting A, Kaleva S, Vehmas T. Emphysema findings associated with heavy asbestos-exposure in high resolution computed tomography of finnish construction workers. Journal of occupational health. 2004;46(4):266-71.
7. Meijer E, Nij ET, Kraus T, van der Zee J, van Delden O, van Leeuwen M, et al. Pneumoconiosis and emphysema in construction workers: results of HRCT and lung function findings. Occupational and environmental medicine. 2011;68(7):542-6.
8. Gevenois P-A, Sergent G, De Maertelaer V, Gouat F, Yernault JC, De Vuyst P. Micronodules and emphysema in coal mine dust or silica exposure: relation with lung function. European Respiratory Journal. 1998;12(5):1020-4.
9. Marchetti N, Garshick E, Kinney GL, McKenzie A, Stinson D, Lutz SM, et al. Association between occupational exposure and lung function, respiratory symptoms, and high-resolution computed tomography imaging in COPDGene. American journal of respiratory and critical care medicine. 2014;190(7):756-62.
10. Choi S, Hoffman EA, Wenzel SE, Tawhai MH, Yin Y, Castro M, et al. Registration-based assessment of regional lung function via volumetric CT images of normal subjects vs. severe asthmatics. Journal of applied physiology. 2013;115(5):730-42.
11. Choi S, Hoffman EA, Wenzel SE, Castro M, Fain S, Jarjour N, et al. Quantitative computed tomographic imaging–based clustering differentiates asthmatic subgroups with distinctive clinical phenotypes. Journal of Allergy and Clinical Immunology. 2017;140(3):690-700. e8.
12. Choi S, Haghighi B, Choi J, Hoffman EA, Comellas AP, Newell JD, et al. Differentiation of quantitative CT imaging phenotypes in asthma versus COPD. BMJ open respiratory research. 2017;4(1):e000252.
13. Parsons L, editor Reducing bias in a propensity score matched-pair sample using greedy matching techniques. Proceedings of the twenty-sixth Annual SAS users group international conference 2001; 2001: SAS Institute Inc.
14. Kim S, Lim M-N, Hong Y, Han S-S, Lee S-J, Kim WJ. A cluster analysis of chronic obstructive pulmonary disease in dusty areas cohort identified three subgroups. BMC pulmonary medicine. 2017;17(1):209.
15. Han Y, Heo Y, Hong Y, Kwon SO, Kim WJ. Correlation between Physical Activity and Lung Function in Dusty Areas: Results from the Chronic Obstructive Pulmonary Disease in Dusty Areas (CODA) Cohort. Tuberculosis and respiratory diseases. 2019;82(4):311-8.
16. Kalačić I. Chronic nonspecific lung disease in cement workers. Archives of Environmental Health: An International Journal. 1973;26(2):78-83.
17. Kim SS, Jin GY, Li YZ, Lee JE, Shin HS. CT quantification of lungs and airways in normal Korean subjects. Korean journal of radiology. 2017;18(4):739-48.
18. Miller MR, Hankinson J, Brusasco V, Burgos F, Casaburi R, Coates A, et al. Standardisation of spirometry. European respiratory journal. 2005;26(2):319-38.
19. Galbán CJ, Han MK, Boes JL, Chughtai KA, Meyer CR, Johnson TD, et al. Computed tomography–based biomarker provides unique signature for diagnosis of COPD phenotypes and disease progression. Nature medicine. 2012;18(11):1711.

20. Choi S, Hoffman EA, Wenzel SE, Castro M, Fain SB, Jarjour NN, et al. Quantitative assessment of multiscale structural and functional alterations in asthmatic populations. Journal of applied physiology. 2015;118(10):1286-98.
21. Zhang Z, Kim HJ, Lonjon G, Zhu Y. Balance diagnostics after propensity score matching. Annals of translational medicine. 2019;7(1).
22. Choi S, Hoffman EA, Wenzel SE, Castro M, Lin C-L. Improved CT-based estimate of pulmonary gas trapping accounting for scanner and lung-volume variations in a multicenter asthmatic study. Journal of Applied Physiology. 2014;117(6):593-603.
23. Smith BM, Hoffman EA, Rabinowitz D, Bleecker E, Christenson S, Couper D, et al. Comparison of spatially matched airways reveals thinner airway walls in COPD. The Multi-Ethnic Study of Atherosclerosis (MESA) COPD Study and the Subpopulations and Intermediate Outcomes in COPD Study (SPIROMICS). Thorax. 2014;69(11):987-96.
24. Fell AKM, Notø H, Skogstad M, Nordby K-C, Eduard W, Svendsen MV, et al. A cross-shift study of lung function, exhaled nitric oxide and inflammatory markers in blood in Norwegian cement production workers. Occup Environ Med. 2011;68(11):799-805.
25. Shim SS, Schiebler ML, Evans MD, Jarjour N, Sorkness RL, Denlinger LC, et al. Lumen area change (Delta Lumen) between inspiratory and expiratory multidetector computed tomography as a measure of severe outcomes in asthmatic patients. Journal of Allergy and Clinical Immunology. 2018;142(6):1773-80. e9.
26. Lambert AR, O'shaughnessy PT, Tawhai MH, Hoffman EA, Lin C-L. Regional deposition of particles in an image-based airway model: large-eddy simulation and left-right lung ventilation asymmetry. Aerosol Science and Technology. 2011;45(1):11-25.
27. Usmani OS, Biddiscombe MF, Barnes PJ. Regional lung deposition and bronchodilator response as a function of β2-agonist particle size. American journal of respiratory and critical care medicine. 2005;172(12):1497-504.
28. Sahu S, Tiwari M, Bhangare R, Pandit G. Particle size distribution of mainstream and exhaled cigarette smoke and predictive deposition in human respiratory tract. Aerosol Air Qual Res. 2013;13(1):324-32.
29. Hoesein FAM, de Hoop B, Zanen P, Gietema H, Kruitwagen CL, van Ginneken B, et al. CT-quantified emphysema in male heavy smokers: association with lung function decline. Thorax. 2011;66(9):782-7.
30. Ashraf H, Lo P, Shaker SB, de Bruijne M, Dirksen A, Tønnesen P, et al. Short-term effect of changes in smoking behaviour on emphysema quantification by CT. Thorax. 2011;66(1):55-60.
31. Kim N, Seo JB, Song K-S, Chae EJ, Kang S-H. Semi-automatic measurement of the airway dimension by computed tomography using the full-width-half-maximum method: a study on the measurement accuracy according to the CT parameters and size of the airway. Korean J Radiol. 2008;9(3):226-35.
32. Sieren JP, Newell Jr JD, Barr RG, Bleecker ER, Burnette N, Carretta EE, et al. SPIROMICS protocol for multicenter quantitative computed tomography to phenotype the lungs. American journal of respiratory and critical care medicine. 2016;194(7):794-806.
33. Cho HB, Chae KJ, Jin GY, Choi J, Lin C-L, Hoffman EA, et al. Structural and functional features on quantitative chest computed tomography in the Korean Asian versus the White American healthy non-smokers. Korean journal of radiology. 2019;20(7):1236-45.

Tables

Table 1. Scanners and scanning protocol used for non-dust-exposed subjects and dust-exposed subjects

	Non-dust-exposed subjects	Dust-exposed subjects
Institution	CNUH	KNUH
Scanner make	Siemens Definition Flash 128 slices	Siemens Definition AS 64 slices
Scan type	Spiral	Spiral
Rotation time(s)	0.5	0.5
Detector configuration	128 × 0.6 mm	64 × 0.6 mm
Pitch	1	1
Peak kilovoltage, kVp	120	140
mAs	110, Effective	100, Effective
Dose modulation	Care dose OFF	Care dose OFF
Reconstruction algorithm	B35f	B30f
Thickness (mm)	1	0.6
Iterative reconstruction	No selection	No selection

CNUH, Chonbuk National University Hospital; KNUH, Kangwon National University Hospital; mAs, milliamperage seconds

Table 2. Propensity score matching before and after data using demographic (sex, age, height, smoking status, and pack-years) information for non-dust-exposed subjects and dust-exposed subjects

	Before propensity score matching					After propensity score matching (1:4)				
	NDE subjects (N=255)		DE subjects (N=66)		St.Diff.	NDE subjects (N=164)		DE subjects (N=41)		St.Diff.
	N	(%)	N	(%)		N	(%)	N	(%)	
Sex										
Male	99	(38.8)	45	(68.2)	61.6	80	(48.8)	20	(48.8)	0.0
Female	156	(61.2)	21	(31.8)		84	(51.2)	21	(51.2)	
Age										
mean±std	51.0	±15.1	70.5	±7.5	±1.6	49.7	±15.4	70.0	±8.0	±1.7
Height										
mean±std	161.4	±9.6	159.9	±10.1	±0.2	162.9	±9.7	157.9	±11.3	±0.5
Smoking										
Non/Former Smoking Participants	224	(87.8)	57	(86.4)	4.4	144	(87.8)	36	(87.8)	0.0
Current Smoking Participants	31	(12.2)	9	(13.6)		20	(12.2)	5	(12.2)	
Pack-years										
mean±std	4.6	±13.2	14.7	±21.9	±0.6	4.4	±12.3	10.4	±22.7	±0.3
BMI										
mean±std	-		-		-	24.4	±3.3	24.1	±2.8	0.372*

NDE, non-dust exposed; DE, dust exposed; St. Diff., standardized differences; *, P-value obtained by one-sample t-test.

Table 3. Comparison of deformation ratios of the bifurcation angle (ε^{θ}) between non-dust-exposed subjects and dust-exposed subjects.

Region	NDE subjects (n = 164)	DE subjects (n = 41)	*P* value
Trachea	-2.713 (7.232)	-1.713 (5.389)	0.191
RMB	14.51 (10.44)	8.172 (6.396)	<0.001
TriRUL	1.290 (12.31)	4.194 (7.858)	<0.05
BronInt	-2.171 (13.53)	-1.849 (11.07)	0.815
LMB	11.29 (10.40)	7.728 (12.39)	<0.01
TriLUL	6.366 (9.857)	2.708 (9.361)	<0.005
LLB6	6.505 (13.91)	5.084 (10.14)	0.266

Values are presented as mean (SD); BronInt, bronchus intermedius; LMB, left main bronchus; RMB, right main bronchus; TriRUL, trifurcation of right lower lobe; TriLUL, trifurcation of left upper lobe; ε^{θ}, deformation ratio of bifurcation angle.

Table 4. QCT-based lung functions between non-dust-exposed subjects and dust-exposed subjects.

QCT-based lung functions		NDE subjects (n = 184)		DE subjects (n =46)		*P* value
TLC, liter		3.902	(1.030)	3.477	(0.970)	<0.001
FRC, liter		2.163	(0.705)	1.977	(0.741)	<0.05
IC, liter		1.794	(0.842)	1.543	(0.723)	<0.005
Jacobian	Total	1.690	(0.364)	1.617	(0.348)	0.058
	LUL	1.601	(0.346)	1.558	(0.355)	0.258
	LLL	1.884	(0.452)	1.900	(0.469)	0.734
	RUL	1.581	(0.338)	1.440	(0.268)	<0.001
	RML	1.465	(0.256)	1.391	(0.224)	<0.005
	RLL	1.861	(0.436)	1.834	(0.414)	0.562
Emph%		0.017	(0.023)	0.010	(0.013)	<0.005
fSAD%		0.087	(0.116)	0.080	(0.106)	0.554

Values are presented as mean (SD); Emph%, percent emphysema; FRC, functional residual volume; fSAD%, percent functional small airway disease; IC, inspiratory capacity; TLC, total lung capacity; QCT, quantitative computed tomography; LLL, left lower lobe; LUL, left upper lobe; RLL, right lower lobe; RML, right middle lobe; RUL, right upper lobe; The values are presented with absolute values in TLC, FRC, and IC, not predicted values.

Figures

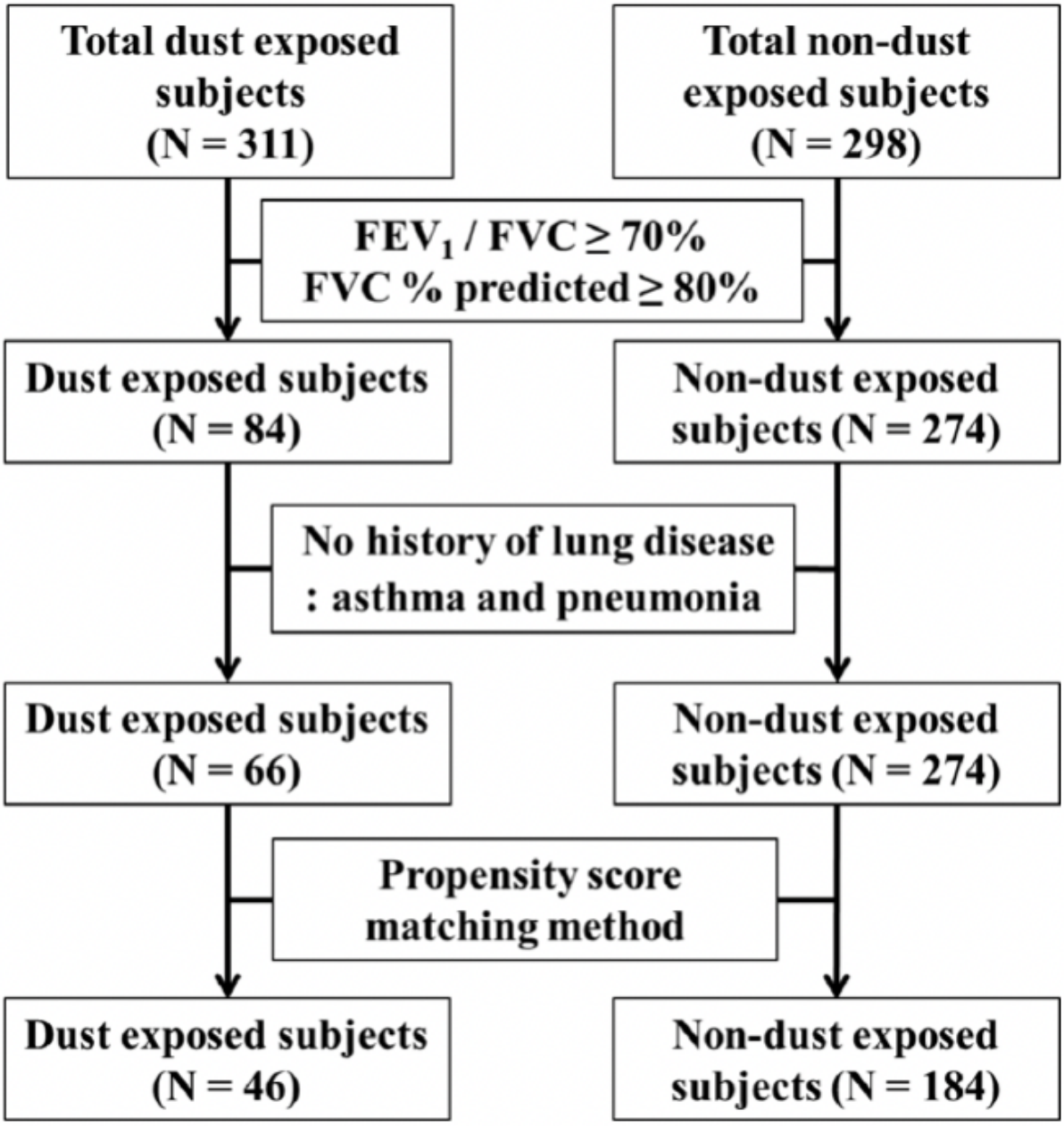

Figure 1

Flow chart of subject selection for dust-exposed subjects and non-dust-exposed subjects. FEV1, forced expiratory volume in 1 second; FVC, forced vital capacity;

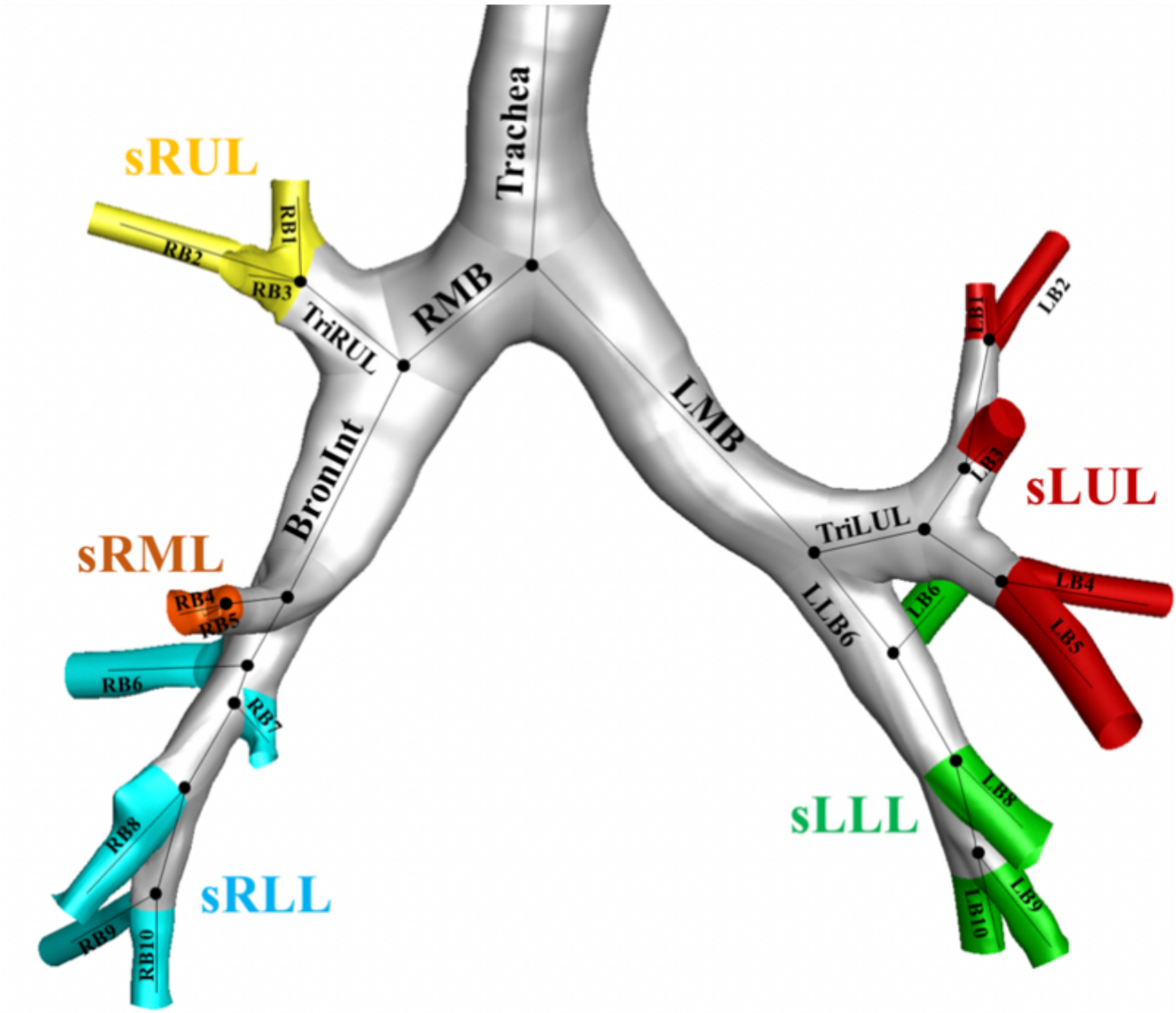

Figure 2

Labels of 26 segmental airways and 5 subgroups of lobes. BronInt, bronchus intermedius; LMB, left main bronchus; RMB, right main bronchus; sLLL, subgrouped left lower lobe including branches of LB6 and LB8 to LB10; sLUL, subgrouped left upper lobe including branches of LB1 to LB5; sRLL, subgrouped right lower lobe including branches of RB6 to RB10; sRML, subgrouped right middle lobe including branches of RB4 and RB5; sRUL, subgrouped right upper lobe including branches of RB1 to RB3; TriLUL, trifurcation of left upper lobe; TriRUL, trifurcation of right upper lobe.

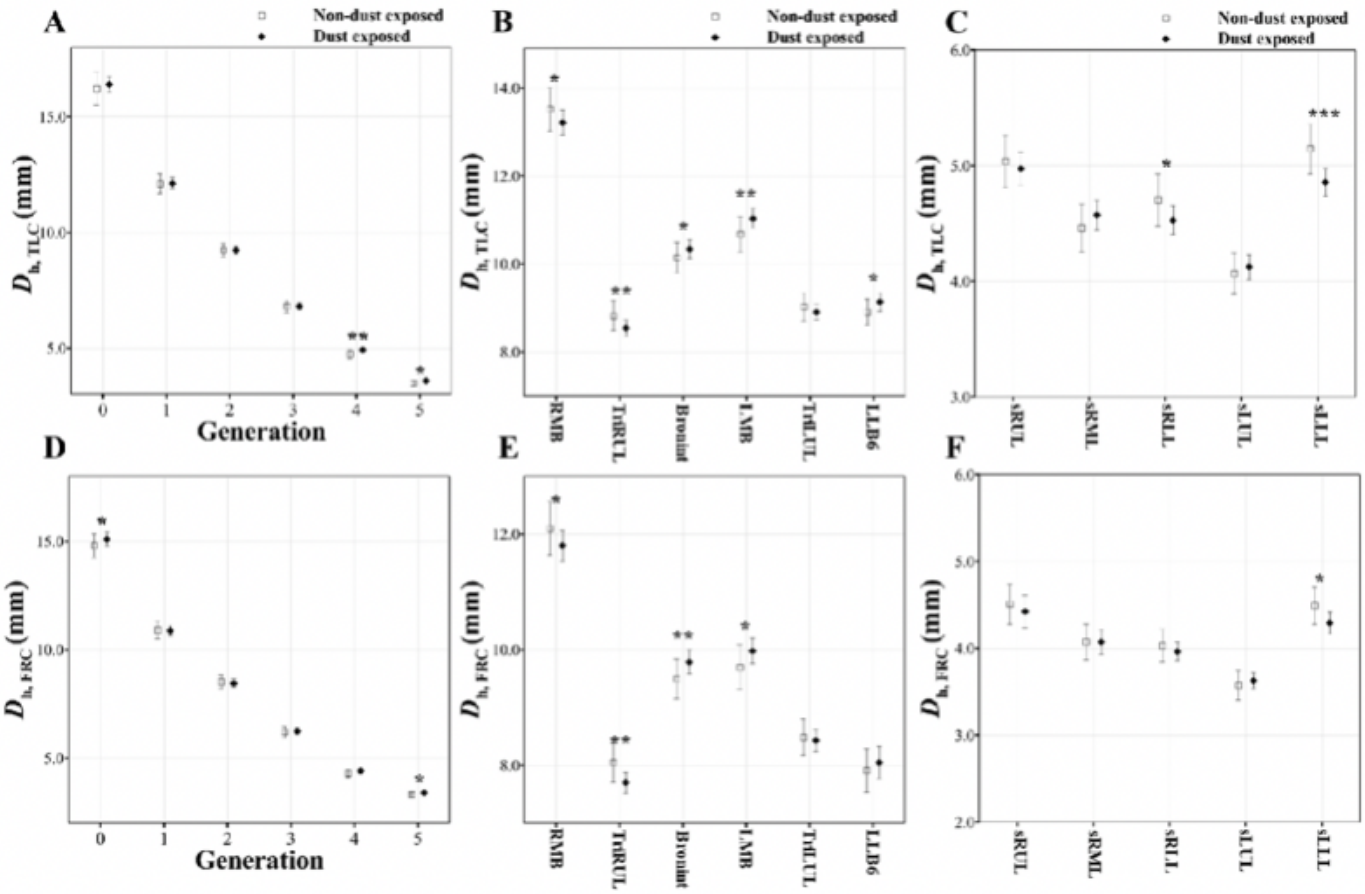

Figure 3

Comparison of luminal hydraulic diameter (Dh) at TLC (A, B, and C) and FRC scans (D, E, and F) between non-dust-exposed subjects and dust-exposed subjects. Values are presented as mean (CI); *P<0.05; **P<0.01; ***P<0.001. Generation zero is started from trachea. BronInt, bronchus intermedius; Dh, hydraulic diameter; FRC, functional residual capacity; LMB, left main bronchus; RMB, right main bronchus; sLLL, subgrouped left lower lobe; sLUL, subgrouped left upper lobe; sRLL, subgrouped right lower lobe; sRML, subgrouped right middle lobe; sRUL, subgrouped right upper lobe; TLC, Total lung capacity; TriLUL, trifurcation of left upper lobe; TriRUL, trifurcation of right upper lobe.

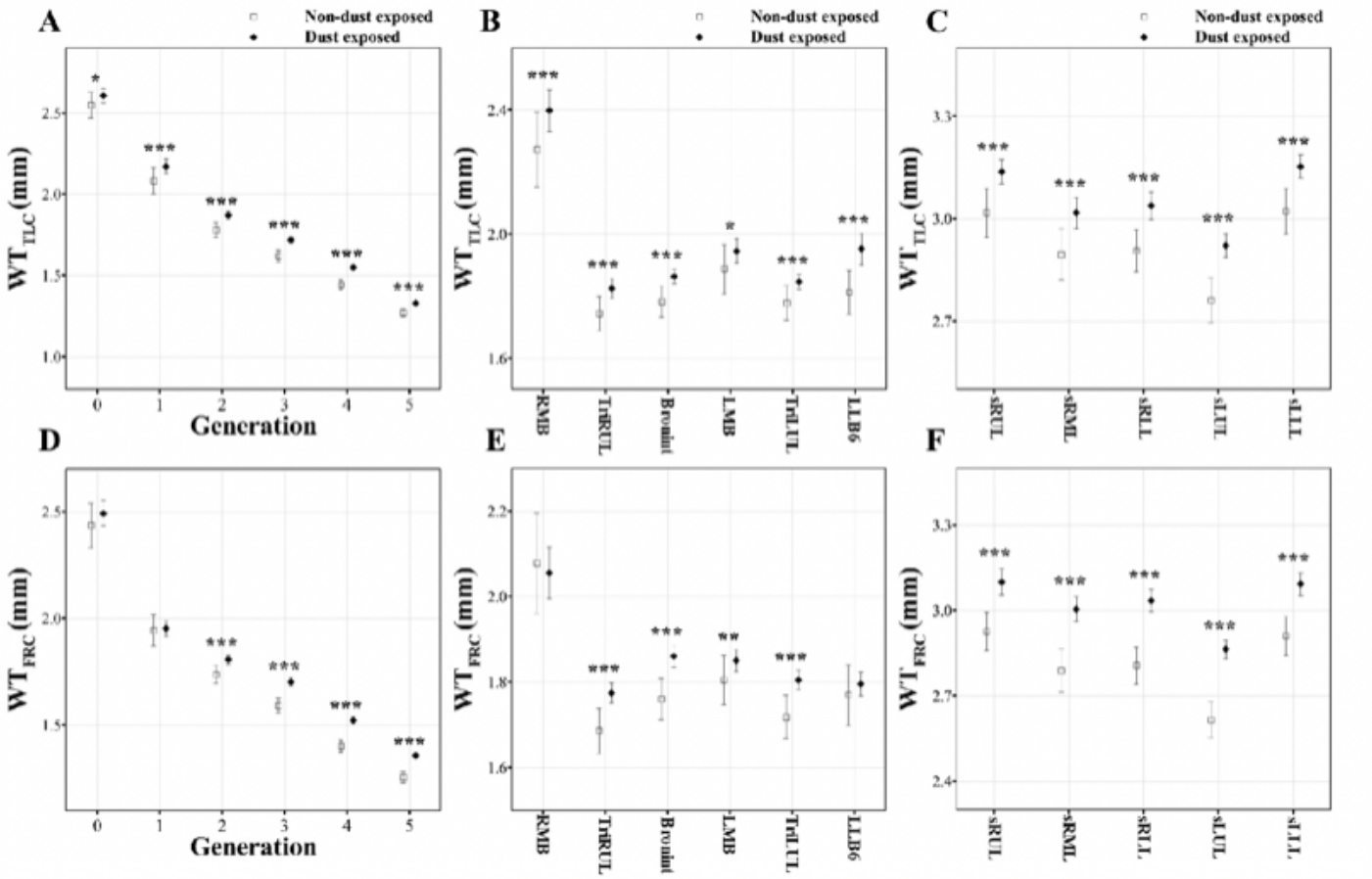

Figure 4

Comparison of wall thickness (WT) at TLC (A, B, and C) and FRC scans (D, E, and F) between non-dust-exposed subjects and dust-exposed subjects. Values are presented as mean (CI); *P<0.05; **P<0.01; ***P<0.001. Generation zero is started from trachea. BronInt, bronchus intermedius; FRC, functional residual capacity; LMB, left main bronchus; RMB, right main bronchus; sLLL, subgrouped left lower lobe; sLUL, subgrouped left upper lobe; sRLL, subgrouped right lower lobe; sRML, subgrouped right middle lobe; sRUL, subgrouped right upper lobe; TLC, total lung capacity; TriLUL, trifurcation of left upper lobe; TriRUL, trifurcation of right upper lobe.

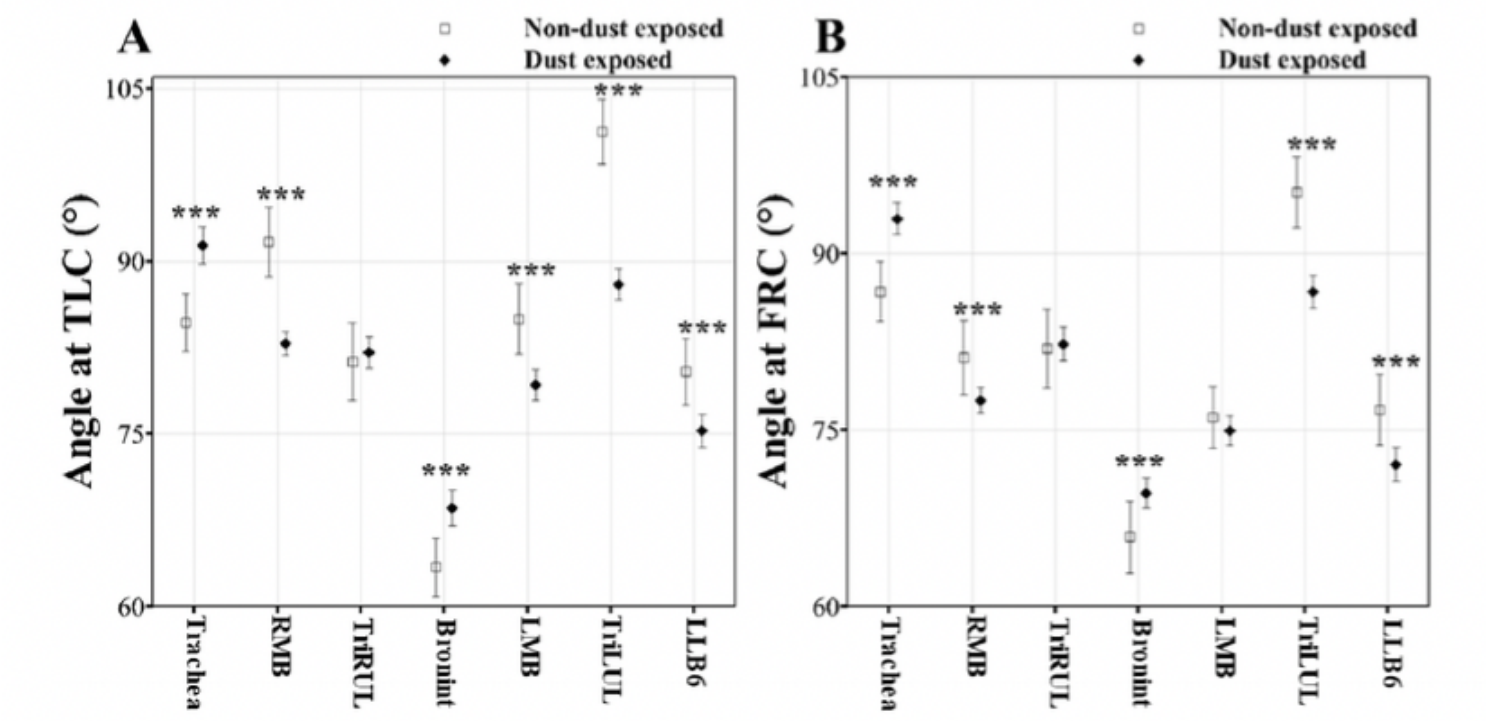

Figure 5

Comparison of airway bifurcation angle (θ) at TLC (A) and FRC (B) scans between non-dust-exposed subjects and dust-exposed subjects. Values are presented as mean (CI); *P<0.05; **P<0.01; ***P<0.001. BronInt, bronchus intermedius; FRC, functional residual capacity; LMB, left main bronchus; RMB, right main bronchus; TLC, total lung capacity; TriLUL, trifurcation of left upper lobe; TriRUL, trifurcation of right upper lobe.

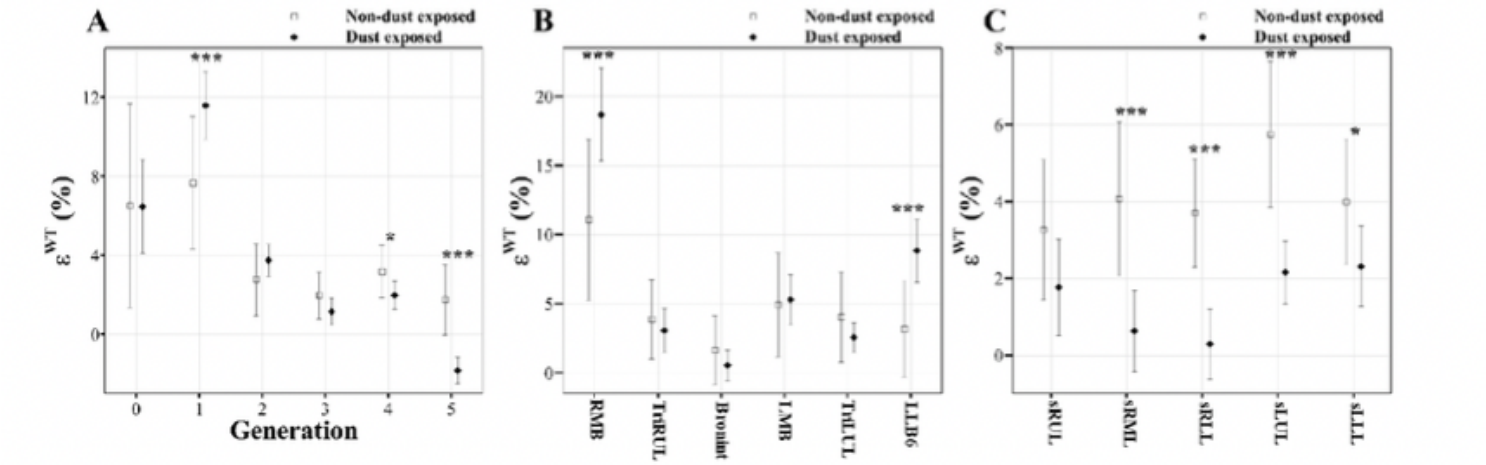

Figure 6

Comparison of deformation ratio of wall thickness (εWT) between non-dust-exposed subjects and dust-exposed subjects. Values are presented as mean (CI); *P<0.05; **P<0.01; ***P<0.001. Generation zero is started from trachea. BronInt, bronchus intermedius; FRC, functional residual capacity; LMB, left main bronchus; RMB, right main

bronchus; sLLL, subgrouped left lower lobe; sLUL, subgrouped left upper lobe; sRLL, subgrouped right lower lobe; sRML, subgrouped right middle lobe; sRUL, subgrouped right upper lobe; TLC, total lung capacity; TriLUL, trifurcation of left upper lobe; TriRUL, trifurcation of right upper lobe.

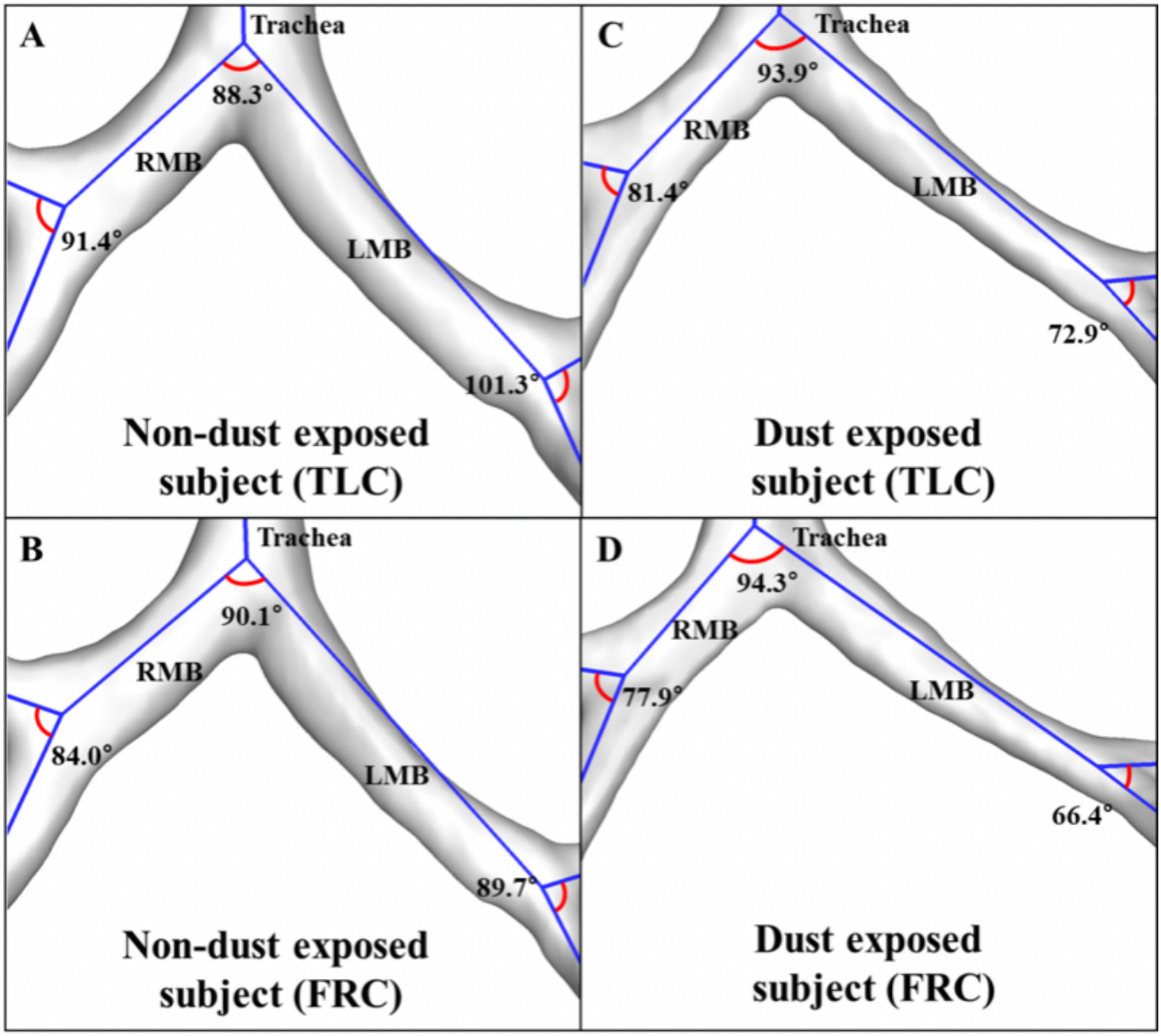

Figure 7

Bifurcation angle of airway in a non-dust-exposed subject at TLC (A) and FRC (B) scans and a dust-exposed subject at TLC (C) and FRC (D) scans. FRC, functional residual capacity; LMB, left main bronchus; RMB, right main bronchus; TLC, total lung capacity.

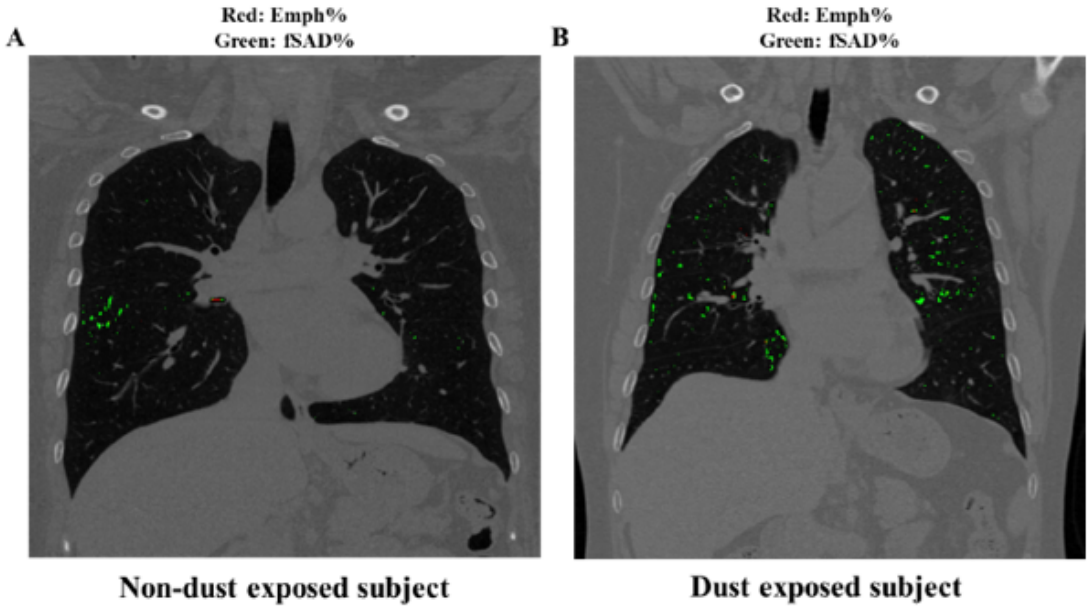

Figure 8

Parenchymal features of Emph% and fSAD% in a non-dust-exposed subject (A) and a dust-exposed subject (B).

Supplementary Files

This is a list of supplementary files associated with this preprint. Click to download.

- Supplementarymaterial20200518.docx
- Methods.docx